Experiments on Fission Dynamics with Relativistic Heavy-Ion Beams

K.-H. Schmidt,[*,a] **P. Armbruster,**[a] **J. Benlliure,**[b] **C. Böckstiegel,**[c] **A. Botvina,**[a,†]

H.-G. Clerc,[c] **T. Enqvist,**[d] **A. Grewe,**[c] **A. Heinz,**[‡,a] **A. R. Junghans,**[§,a] **B. Jurado,**[a]

J. Müller,[c] **V. Ricciardi,**[a] **F. Rejmund,**[e] **S. Steinhäuser,**[c] **and B. Voss**[a]

[a] *GSI, Planckstr. 1, 64291 Darmstadt, Germany*

[b] *University of Santiago de Compostela, 15706 Santiago de Compostela, Spain*

[c] *IKDA, TU Darmstadt, Schloßgartenstr. 9, 64289 Darmstadt, Germany*

[d] *University of Jyväskylä, 40351 Jyväskylä, Finland*

[e] *IPN Orsay, IN2P3, 91406 Orsay, France*

[Abstract] At GSI, Darmstadt, an experimental program on fission with relativistic heavy-ion beams is in progress. A large range of excitation energies, combined with low angular momentum and small shape distortion is accessible. Full nuclide identification of the reaction residues is achieved by applying inverse kinematics. The nuclide production and the kinematics of fission fragments from a variety of primordial and radioactive projectiles reveal new insight into the influence of shell effects and dissipation on the fission process. The present contribution gives an overview on the experimental methods, the experimental results and the prospects for future progress.

1 Introduction

Nuclear fission as a prototype of a non-equilibrium dynamical process of a mesoscopic system of fermions is not yet fully understood. To most part, this is due to the lack of experimental knowledge obtained so far in conventional experiments. These experiments were restricted in the choice of the system, in the control of the relevant pa-

---

[*] Corresponding author, E-mail: k.h.schmidt@gsi.de, Fax: +49 6159 71 2785, www-wnt.gsi.de/kschmidt
[†] Permanent address: Inst. for Nuclear Research, Russian Academy of Sciences, 117312 Moscow, Russia
[‡] Present address: Argonne Nat. Lab., Physics Div., 9700 South Cass Avenue, Argonne, IL 60439, U.S.A.
[‡] Present address: Nucl. Phys. Lab., BOX 354290, University of Washington, Seattle, WA 98195, U.S.A.

rameters like excitation energy, angular momentum and shape, and in the measurable quantities.

Low-energy fission could only be studied using primordial or long-lived target materials. With the exception of some spontaneously fissioning nuclei, this limited the investigations to a few species in the vicinity of the available target nuclides.

Fission from high excitation energies, mostly studied in heavy-ion reactions at beam energies around 5 to $20A$ MeV, suffered from two problems: Firstly, high excitation energies were accompanied with broad angular-momentum distribution. Secondly, the reaction dynamics started with large shape distortions.

Generally, the full identification of the fission fragments in nuclear charge and mass is a difficult task, due to the low fission-fragment velocities. This goal has only been reached in a few thermal-neutron-induced fission reactions for nuclei in the light group of the fission fragments. In fission from high excitation energies, the full nuclide identification in-flight has never been achieved.

This contribution gives an overview on the results of first experiments performed at GSI, using relativistic beams of primordial and radioactive fissile nuclei, in which several of the previous restrictions could be overcome.

2 Experiment

2.1 Accelerator and spectrometer

Two installations of GSI, Darmstadt, are most essential for the experiments we report on in the present contribution: The heavy-ion synchrotron SIS18 accelerates heavy ions up to uranium to energies of at least $1A$ GeV, and the fragment separator [1], shown in Figure 1, allows determining the magnetic rigidity of the reaction products emerging from a target mounted at its entrance with high resolution.

2.2 Full identification of one fission fragment

Using relativistic beams of primordial nuclides, one product emerging from the reaction can be analyzed with the fragment separator used as a high-resolution spectrometer [2,3,4]. The magnetic rigidity, combined with the energy loss and time-of-flight [5],

measured with dedicated detectors, allows fully identifying this reaction product in nuclear charge and mass. In addition, its longitudinal momentum is measured with high precision. It is essential that the ions are fully stripped at the relativistic energies. Thus, their nuclear charge can be deduced from the measured energy loss in an ionization chamber with high resolution [6]. Figure 2 demonstrates the resolution in mass number and nuclear charge in a typical example.
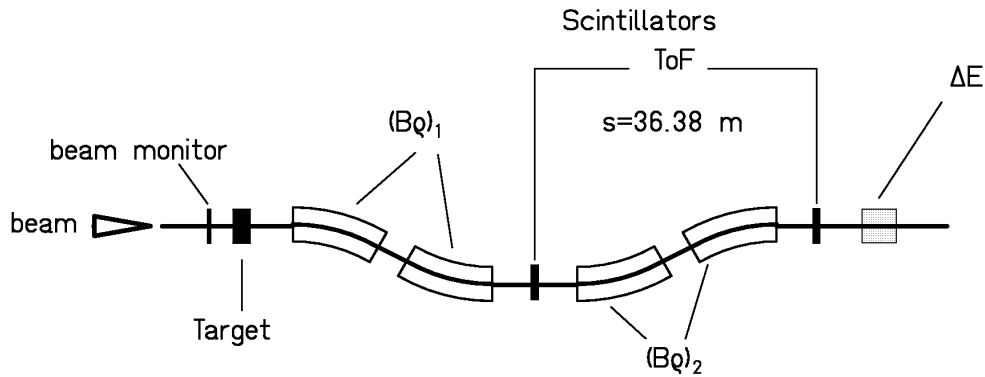

Figure 1: Schematic presentation of the fragment separator and the main detectors.

2.3 Simultaneous measurement of both fission fragments

In another full-acceptance experiment, both fission fragments are simultaneously registered in a large double ionization chamber and a time-of-flight section [7], and their nuclear charges and velocity vectors were determined. The experimental set up is shown in Figure 3. Beams of primordial and radioactive nuclei from the fragment separator have been used. As important information to distinguish between different reaction mechanisms, i.e. electromagnetic- or nuclear-induced fission, the nuclear charge of the fissioning system could be determined from the nuclear charges of the fission fragments, which were again measured with high precision. A two-dimensional cluster plot of the energy loss recorded in the two parts of the double ionization chamber is depicted in Figure 4.
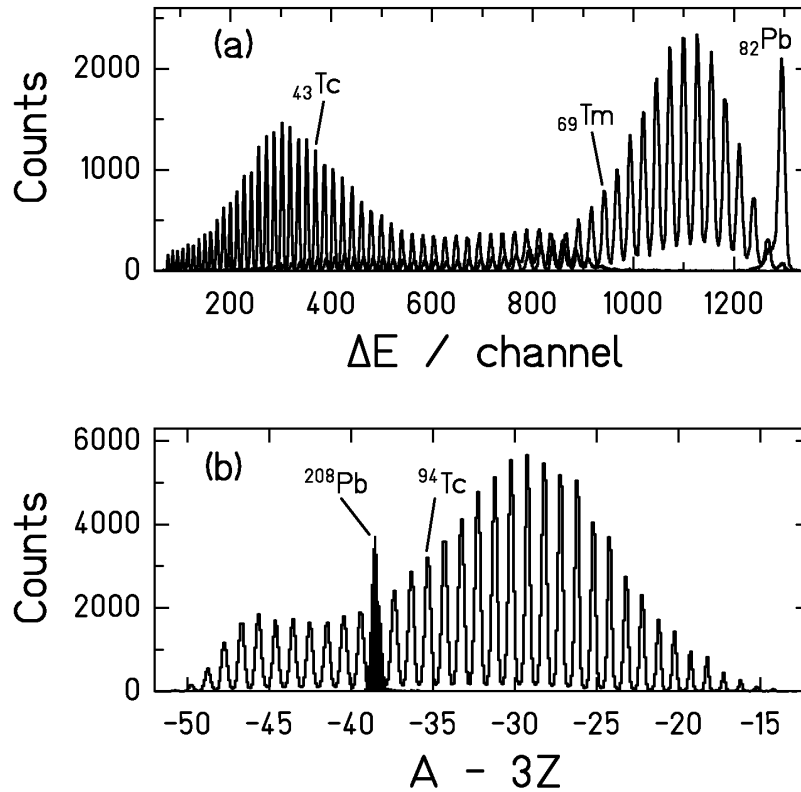
Figure 2: Example for the resolution in nuclear charge and mass for reaction products of the system ^{1}H + ^{208}Pb at 1A GeV (from Reference [8]). The spectra measured with a few different settings of the spectrometer are overlaid.
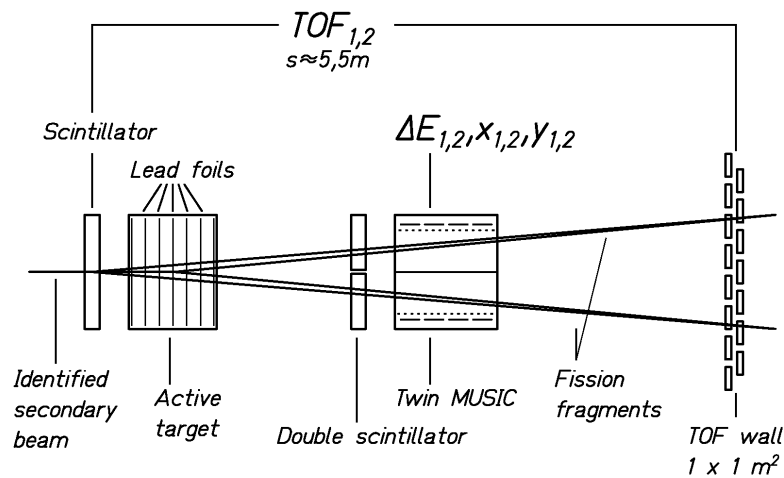

Figure 3: Experimental set up to simultaneously measure both fission fragments produced in inverse kinematics (from Reference [7]).
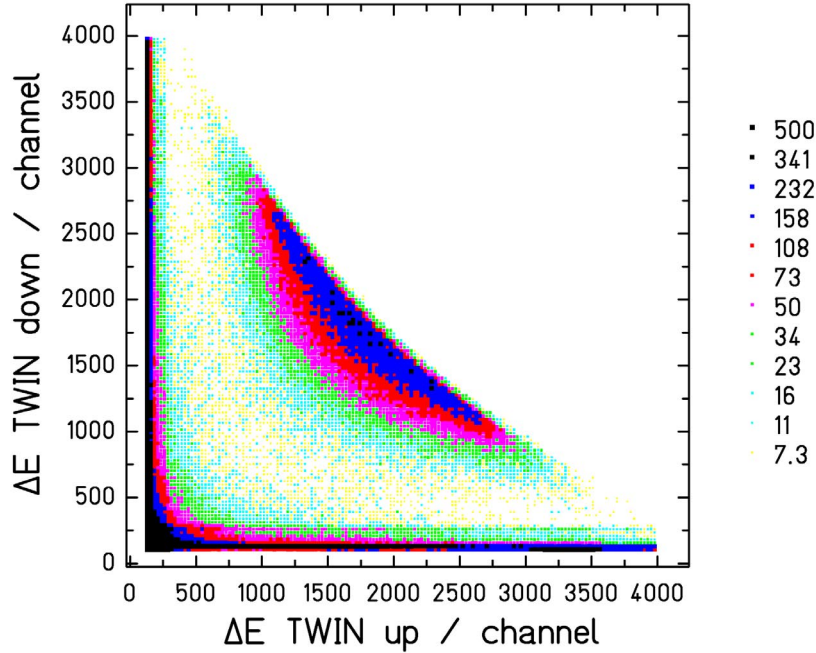
Figure 4: Cluster plot of fission fragments recorded by the double ionization chamber in the reaction $^{238}U + (CH_2)_n$.

2.4 Reaction mechanisms used to induce fission

Heavy-ion collisions at relativistic energies can be classified into different groups. Very peripheral collisions without nuclear contact are governed by electromagnetic forces [9]. Mostly, the giant dipole resonance is excited [7]. The excitation-energy distribution of heavy fissile nuclei peaks at about 11 MeV and has a width of a few MeV. Peripheral collisions with nuclear contact lead to the abrasion of a number of nucleons and induce appreciably higher excitation energies, which amount to 27 MeV on the average per nucleon abraded [10]. With increasing mass loss, the excitation energy of the spectator reaches to very high values, even making it a suitable tool to investigate thermal multifragmentation [11]. For a heavy nucleus, excitation energies of several hundred MeV can be reached with a relative mass loss of only a few percent. Thus, shape distortions after the abrasion phase are small. Due to the lack of momentum transfer to the spectator, the angular momentum induced is rather small, too, in the order of 10 to 20 $\hbar$ on the av-

erage, as deduced from theoretical estimations [12], which are confirmed by experimental results [13]. Thus, the characteristics searched for in anti-proton-induced reactions [14] are even better realized in peripheral heavy-ion collisions.

3 Results and discussion

3.1 Multi-model fission

Multi-model fission of radioactive nuclei was investigated in a dedicated experiment [7]. Relativistic secondary projectiles were produced by fragmentation of a $1A$ GeV ^{238}U primary beam in a beryllium target and identified in nuclear charge and mass number by the fragment separator. According to the impact parameter, some of these secondary projectiles were excited by electromagnetic interactions in a secondary lead target, inducing fission from excitation energies around 11 MeV. The fission fragments were identified in nuclear charge, and their velocity vectors were determined. Elemental yields and total kinetic energies of 70 short-lived nuclear species have been obtained, almost all of them for the first time. In particular, the transition from symmetric to asymmetric fission around ^{227}Th has been covered systematically.

The most important experimental achievements of this secondary-beam experiment were the rather free choice of the nucleus to be investigated, independently of its chemical properties and independently of its radioactive decay characteristics, down to half-lives in the order of 100 ns, the excellent nuclear-charge resolution for all fission fragments, and the remarkably good determination of the mean total kinetic energies with uncertainties in the order of 10^{-5} of the laboratory energies.

The data were analyzed in terms of fission channels [15]. The weights of the three predominant channels, standard I, standard II and superlong, were found to be consistent with the trends of previous results found for heavier actinides [16]. Calculations with a semi-empirical fission model [17] were performed, assuming (i) that the population of the fission channels is determined by the level density above the mass-asymmetry-dependent fission barrier, (ii) that the dynamics from saddle to scission is described by the fission-channel concept [18, 19], and (iii) that the mean values and the widths of charge distribution and total kinetic energy of the fission fragments are finally determined at the scission

configuration. The results are compared to the experimental data in Figure 5. This analysis corroborates the fission-channel concept and reveals the strong influence of phase space on the fission process [7].
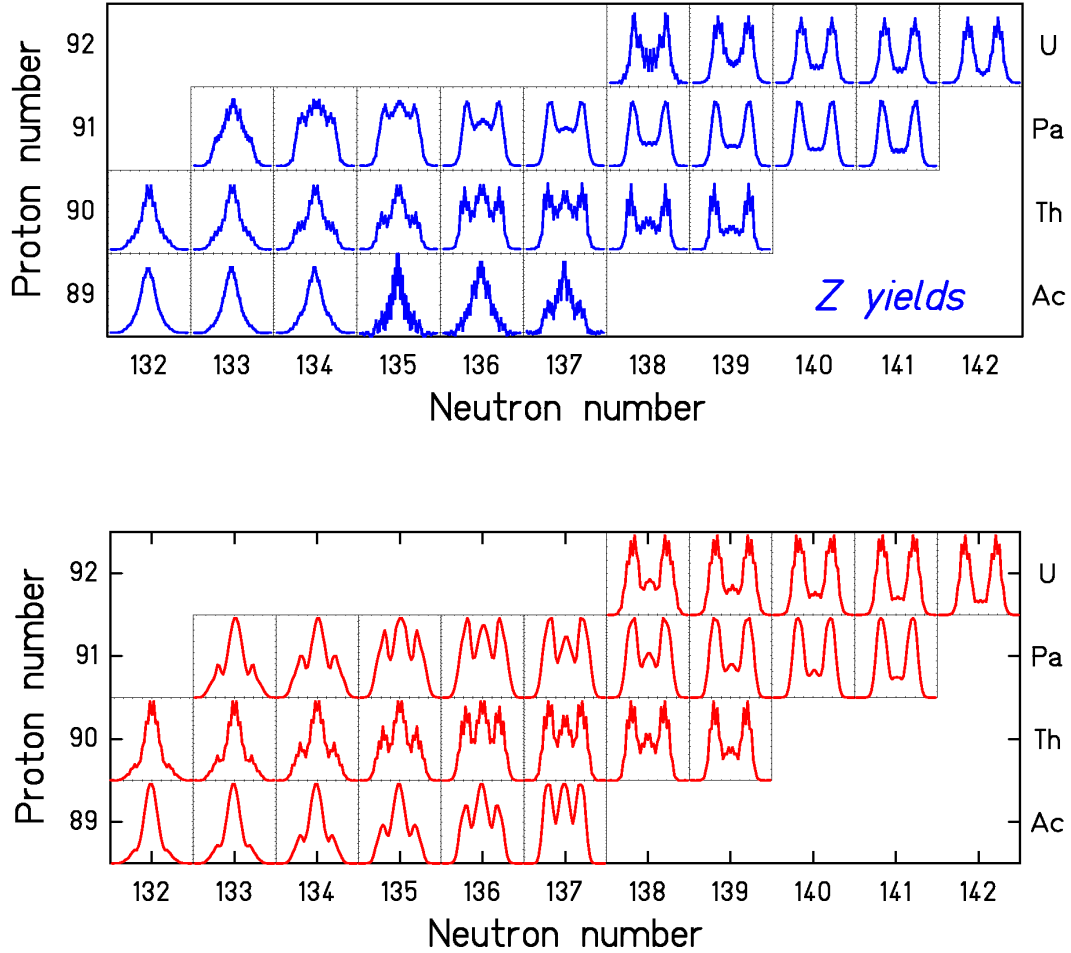

Figure 5: Upper part: Measured nuclear-charge distributions in the transition zone from symmetric to asymmetric fission around ^{227}Th. Lower part: Result of a model calculation as described in the text (from Reference [7]).

3.2 Dissipation

Fission is a unique tool to investigate nuclear dissipation. Our experiments are sensitive to the following features: At low excitation energies, dissipation manifests itself in

the breaking of pairs. At high excitation energies, it reduces the flux over the fission barrier.

3.2.1 Onset of dissipation in a super-fluid nuclear system

The excellent Z resolution achieved in the secondary-beam experiment [7] described in the previous section, allowed investigating pair breaking in fission in a systematic way [20]. Strong even-odd effects in the element yields were found in symmetric charge splits for the first time. A general tendency of the even-odd effects to increase in very asymmetric charge splits was established, even for odd-Z fissioning nuclei. Two representative cases are shown in Figure 6. A new theoretical description [21], based on the statistical model, is able to explain these findings and to deduce the energy dissipation in the fission process, starting from a cold, superfluid system at the barrier down to the scission configuration.
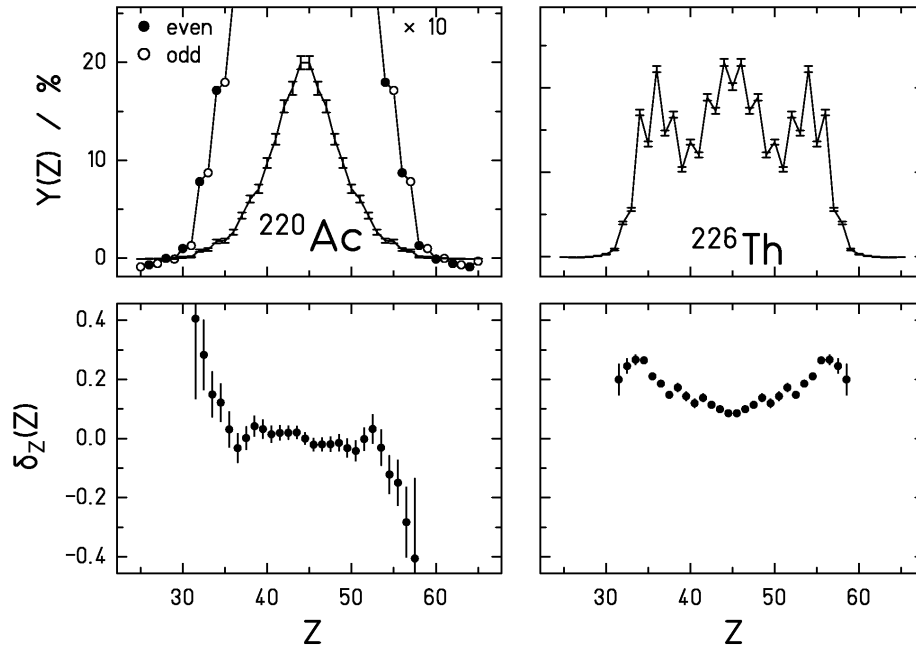

Figure 6: Element yields (upper part) and deduced local even-odd effect as defined in Reference [22] (lower part) for electromagnetic-induced fission of ^{220}Ac and ^{226}Th.

3.2.2 Dissipation in hot nuclei

The properties of the projectile fragments produced in peripheral nuclear collisions are best suited for investigating the influence of dissipation on the fission process. These particular properties allow analyzing the data with the theoretical framework developed by Grangé and Weidenmüller [23], avoiding disturbing influences of high angular momenta or large shape distortions. Besides the total fission cross section (Figure 7), the excellent Z resolution of the experiment allows to introduce two new experimental signatures which are sensitive to dissipation; the width of the element distributions (Figure 8) and the "partial" fission cross sections (Figure 9), both available for specific elements produced as projectile fragments with different initial projectiles. By use of secondary beams, the influence of fissility and excitation energies of the fissioning systems could independently be investigated [24]. The different experimental signatures are sensitive to different things: While the total fission cross sections integrate over all processes, the width of the element distributions particularly measures the mean excitation energy at fission. The partial fission cross sections probe the excitation-energy dependence of the fission probability. All three signatures are rather consistently described by the model calculation with a reduced dissipation coefficient $\beta = 2 \cdot 10^{21}$ s^{-1}, which is close to the critical damping.

The interpretation of these data is still in progress. A major goal is to incorporate a realistic in-grow function, representing the solution of the Fokker-Planck equation, for the time-dependent fission width in the statistical deexcitation code, since previously used approximations [25, 26] were found to lead to erroneous results [27, 28].
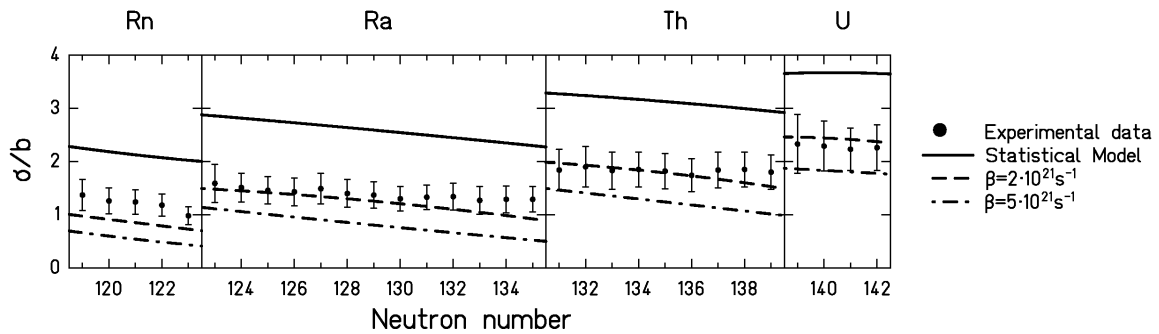

Figure 7: Total nuclear-induced fission cross section of different secondary projectiles of 430A MeV in a lead target compared to model calculations with different options.
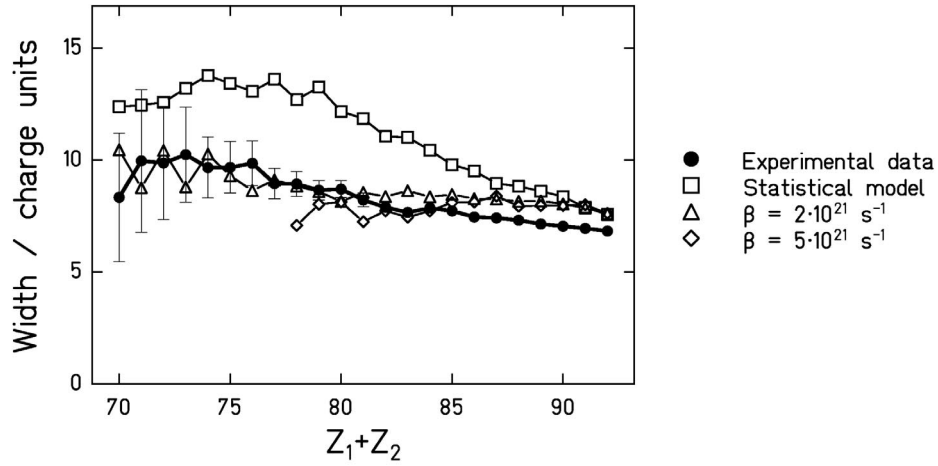
Figure 8: Measured width of the charge distribution of fission fragments from the reaction ^{238}U + $(CH_2)_n$ at $1A$ GeV for given values of $Z_1 + Z_2$ in comparison with model calculations with different parameters.
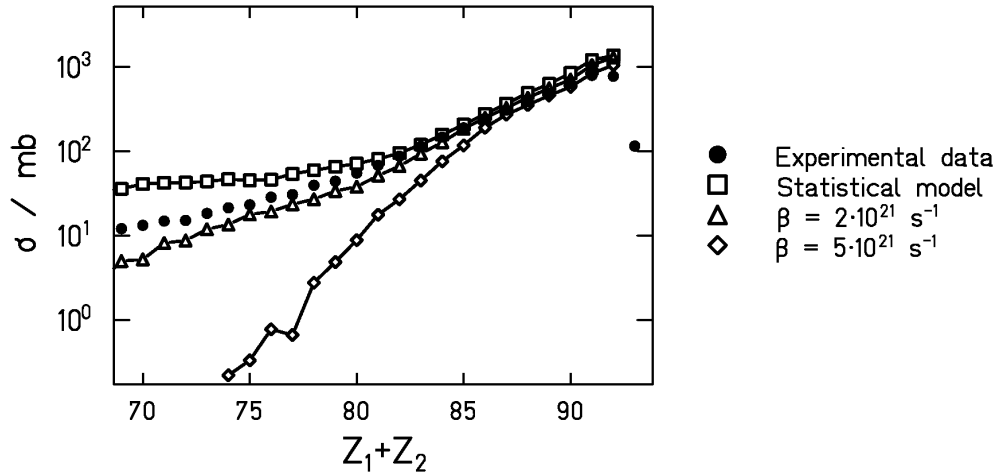

Figure 9: Partial fission cross sections measured in the reaction ^{238}U + $(CH_2)_n$ at $1A$ GeV for given values of $Z_1 + Z_2$ in comparison with model calculations with different parameters.

3.2.3 Temperature limit for sequential decay

The excitation energy induced in the abrasion process as a function of mass loss has been established experimentally [10]: An excitation energy of 27 MeV has been found to be induced by the abrasion of one nucleon. Thus, very high excitation energies can be induced. It is known that very high excitation energies lead to a simultaneous break-up of the system, before the excited fragments decay sequentially [11]. For the analysis of nuclear dissipation, described in the preceding section, one needs to know the initial conditions at the beginning of the statistical deexcitation cascade (the sequential decay) in which fission is part of the competing processes. That means, if there is a break-up phase, we need to know the excitation energy after that phase. Recently, we could deduce the freeze-out temperature T_f after the break-up stage from the isospin thermometer [29], that is, by the variation of the *N*-over-*Z* ratio in the evaporation cascade. We found a value of about $T_f = 5$ MeV, corresponding to $E^*=2.5$ MeV/u in the SMM [32, 33] calculations shown in Figure 10, independently from the projectile and from the size of the fragment. Lower values preserve the neutron excess of the projectile to a larger extent, while higher values tend to approach the EPAX [30] prediction which assumes a universal "evaporation-residue corridor" [31] where the competition between evaporation of protons and neutrons goes into saturation.
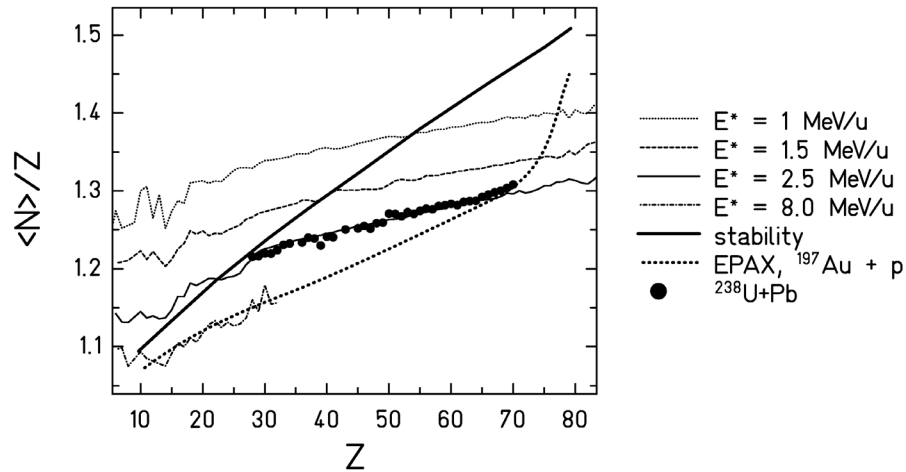

Figure 10: Average *N*-over-*Z* of the projectile fragments from the reaction ^{238}U (1*A* GeV) + Pb [4] compared to SMM [32, 33] calculations with different initial excitation energies. The beta-stability and the prediction of EPAX [30] for ^{197}Au+p are also given.

The assumed break-up density, another important parameter of the SMM calculation, was assumed to be 6 times normal nuclear density. However, it does not have a sizeable influence on the neutron-to-proton ratio of the fragments.

Besides other very interesting consequences, this finding is an important ingredient to deduce the influence of dissipation on the fission process, as described in the preceding section. In addition, it means that fission is prohibited above a temperature of 5 MeV by other than dissipative phenomena, namely by thermal instabilities.

3.3 Extremely asymmetric mass splits

The high-resolution spectrometer is a sensitive tool to investigate fission leading to extremely asymmetric mass splits. We investigated the fission following the spallation of ^{238}U by 1 GeV protons in inverse kinematics [34]. Fission fragments as light as neon could be observed. Their cross sections and their isotopic distributions contain valuable information on the dynamics of fission, e.g. on the charge polarization in extreme mass splits. Figure 11 shows the velocity distributions of sodium, chlorine, and vanadium isotopes produced in the titanium windows and in the hydrogen target itself. While the fragmentation products at mid-velocity are produced in the windows, fission appearing at
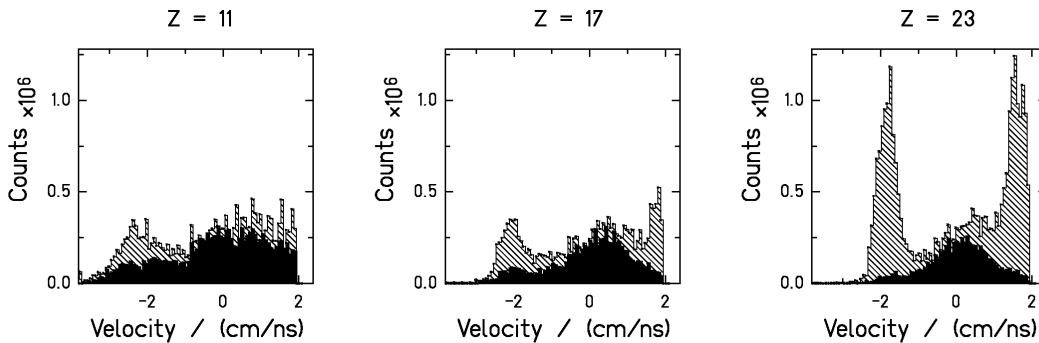

Figure 11: Velocity distribution of detected reaction products from a ^{238}U beam (1A GeV) in titanium (full histogram) and hydrogen (hatched histogram). The counts have been normalized to the same number of projectiles. Due to technical reasons, the spectrum is truncated at +2 cm/ns.

a velocity of 2 cm/ns in forward and backward direction is mostly produced in the hydrogen target. Note that sideward-emitted fission fragments are not transmitted by the fragment separator due to its limited angular acceptance.

In addition, this finding shows for the first time that light nuclides produced at ISOLDE [35] by spallation of uranium-carbide targets by 600 MeV protons, previously considered as "fragmentation" products, result from extremely asymmetric fission of highly excited, heavy spallation products. Indeed, as Figure 12 shows, the measured isotopic distribution of potassium isotopes, identified as fission products in ^{238}U ($1A$ GeV) on proton, perfectly fits to the ISOLDE yields.
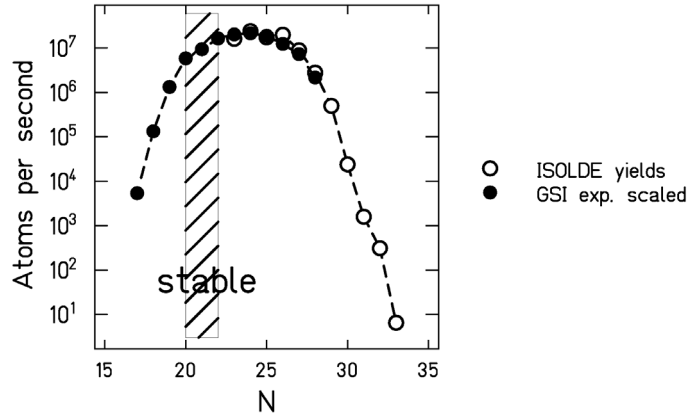

Figure 12: Yields of potassium isotopes measured at ISOLDE [35] in comparison with the isotopic distribution measured in the inverse-kinematics reaction ^{238}U on proton [34].

4 Prospects

In spite the considerable progress achieved in fission experiments by applying inverse kinematics, including the use of secondary beams, several improvements of the experimental technique are desirable. Actually, a new super-conducting analysis magnet is being designed [36], which will allow determining the masses of the fission fragments. When the charged particles are deflected, one can also apply the large-area neutron detector [37] to register the neutrons emitted from the fragments to determine the number of neutrons emitted prior to scission and to deduce the excitation energies of the fragments.

Another goal is a better knowledge of the initial excitation energy of the system, in particular in electromagnetic-induced fission. The excitation by inelastic electron scattering in an electron - heavy-ion - collider ring, which is actually part of the plans for the new GSI facility, would improve the situation considerably.

5 Summary

Experiments in inverse kinematics using relativistic beams of primordial and radioactive species have opened up new possibilities for experimental investigations of nuclear fission by extending the choice of systems to be investigated, by better controlling some relevant parameters like angular momentum and initial shape, and by fully identifying the fission fragments. First results allowed improving our understanding of dissipation from very low to very high excitation energies, the characteristics of multi-modal fission and the occurrence of extremely asymmetric mass splits. Other characteristics of the new experimental technique, however, have not yet reached the standard, occasionally achieved in conventional experiments. In particular it is the goal of new experimental installations actually planned to provide a better definition of the initial excitation energy and to simultaneously detect the emitted light particles.

References

[1] H. Geissel et al., Nucl. Instrum. Meth. B70, 286 (1992).

[2] P. Armbruster et al., Z. Phys. A 355, 191 (1996).

[3] M. de Jong et al., Nucl. Phys. A 628, 479 (1998).

[4] T. Enqvist et al., Nucl. Phys. A 658, 47 (1999).

[5] B. Voss et al., Nucl. Instrum. Meth. A 364, 150 (1995).

[6] M. Pfützner et al., Nucl. Instrum. Meth. B 86, 213 (1994).

[7] K.-H. Schmidt et al., Nucl. Phys. A 693, 169 (2001).

[8] T. Enqvist et al., Nucl. Phys. A 686, 481 (2001).

[9] G. Baur and C. A. Bertulani, Phys. Rev. C 34, 1654 (1986).

[10] K.-H. Schmidt et al., Phys. Lett. B 300, 313 (1993).

[11] J. Pochodzalla and W. Trautmann, in "Isospin Physics in Heavy-Ion Collisions at Intermediate Energies" Nova Science Publishers, Inc.

[12] M. de Jong et al., Nucl. Phys. A 613, 435 (1997).

[13] M. Pfützner et al., submitted to Phys. Rev. C.

[14] F. Goldenbaum et al., Phys. Rev. Lett. 77, 1230 (1996).

[15] K.-H. Schmidt et al., Proc. 2nd Intern. Workshop Nucl. Fission, Seyssin, 1998.

[16] F. Gönnenwein, in "The Nuclear Fission Process", CRC Press, London, 1991, C. Wagemans ed., pp. 409.

[17] J. Benlliure et al., Nucl. Phys. A 628, 458 (1998).

[18] V. V. Pashkevich, Nucl. Phys. A 169, 275 (1971).

[19] U. Brosa, S. Grossmann, A. Müller, Phys. Rep. 197,167 (1990).

[20] S. Steinhäuser et al., Nucl. Phys. A 634, 89 (1998).

[21] F. Rejmund, Nucl. Phys. A 678, 215 (2000).

[22] B. L. Tracy et al., Phys. Rev. C 5, 222 (1972).

[23] P. Grange and H. A. Weidenmüller, Phys. Lett. B 96, 26 (1980).

[24] B. Jurado et al., in Proc. Winter Meeting Nucl. Phys., Bormio, 2001.

[25] E. M. Rastopchin et al., Sov. J. Nucl. Phys. 53, 741 (1991).

[26] R. Butsch et al., Phys. Rev. C 44, 1515 (1991).

[27] B. Jurado et al., Contr. to INPC, Berkeley, 2001.

[28] B. Jurado et al., to be published.

[29] K.-H. Schmidt et al., to be published

[30] K. Sümmerer and B. Blank, Phys. Rev. C 61, 034607 (2000).

[31] J.-P. Dufour et al., Nucl. Phys. A 387, 157c (1982).

[32] A. S. Botvina, A. S. Iljinov, and I. N. Mishustin, Nucl. Phys. A 507, 649 (1990).

[33] J. P. Bondorf, A. S. Botvina, A. S. Iljinov, I. N. Mishustin, and K. Sneppen, Phys. Rep. 257, 133 (1995).

[34] M. V. Ricciardi et al., in Proc. Winter Meeting Nucl. Phys., Bormio, 2001.

[35] H.-J. Kluge, ISOLDE user's guide, CERN 86-05 (1986).

[36] A. Dael et al., Contr. Conf. Magnet Technology 17, Geneva, 2001.

[37] Th. Blaich et al., Nucl. Instrum. Meth. A 314, 136 (1992).